Nazila Gholipour, Mehdi Akhlaghi, Amin Mokhtari Kheirabadi, Mahdi Fasihi Ramandi, Ali Farashahi, Davood Beiki and Amir R. Jalilian*

Development of a novel ^{68}Ga-dextran carboxylate derivative for blood pool imaging

https://doi.org/10.1515/ract-2018-2959
Received March 21, 2018; accepted October 25, 2018

Abstract: To develop a possible PET blood pool imaging agent, a series ^{68}Ga-dextran carboxylate derivatives were prepared. Dextran carboxylates with different degree of oxidations (DO) were prepared through stepwise dextran oxidation using $NaIO_4$ and CH_3COOOH. The products were characterized by FT-IR and GPC, followed by solubility and toxicity tests on Hella cells (viability = 98.6, 97.4 and 95.6 % for 3 dextran carboxylates with DOs: 8.3, 24.6 and 39.8 %, respectively. The products were labeled with ^{68}Ga (radiochemical purity > 98 %; ITLC) followed by stability tests in final solution as well as in presence of cycteine and human serum. Two stable tracers (DOs; 24.6 and 39.8 %) were adminstered intravenously into wild type rat tail vein separately demonstrating suitable retention in circulation as expected from blood pool imaging agents. Liver and spleen also contained activities. The major excretion was through urinary pathway *esp.* for derivative with DO. 39.8 %. Unlike ^{68}Ga-dextran, lungs showed lower uptake. The dextran carboxylate with the highest 39.8 % showed the best characteristics for a blood pool agent, though more studies including PET imaging in larger mammals are required.

Keywords: Gallium-68, dextran carboxylate, radiolabeling, blood pool agents, toxicity, biodistribution.

***Corresponding author: Amir R. Jalilian,** Tehran University of Medical Sciences, Research Center for Nuclear Medicine, Shariati Hospital, North Kargar Ave., P.O. Box: 1414713135, Tehran, Iran, Tel.: 0098 21 88633333, Fax: 0098 21 88026905, E-mail: jalilian1971@gmail.com
Nazila Gholipour: Chemical Injuries Research Center, Systems Biology and Poisonings Institute, Baqiyatallah University of Medical Sciences, Tehran, Iran; and Faculty of Pharmacy, Baqiyatallah University of Medical Sciences, Tehran, Iran
Mehdi Akhlaghi, Amin Mokhtari Kheirabadi and Davood Beiki: Research Center for Nuclear Medicine, Tehran University of Medical Sciences, Tehran, Iran
Mahdi Fasihi Ramandi: Molecular Biology Research Center, System Biology and Poisonings Institute, Baqiyatallah University of Medical Sciences, Tehran, Iran
Ali Farashahi: Tehran Heart Center, Tehran University of Medical Sciences, Tehran, Iran

1 Introduction

Positron emission tomography (PET) has shown great impact on the visualizing of physiological processes in human being thanks to the development of various radiopharmaceuticals. Several positron emitters such as ^{18}F ($T_{1/2}$ = 109.74 min) [1], ^{64}Cu ($T_{1/2}$ = 12.70 h) [2], ^{89}Zr ($T_{1/2}$ = 78.42 h) [3] and ^{68} Ga ($T_{1/2}$ = 67.71 min) [4] have been used in the development of successful radiopharmaceuticals. Among those, ^{68}Ga has shown desirable chemical and physical characteristics especially due to availability from pharmaceutical grade ^{68}Ge/^{68}Ga generator, suitable half-life and possibility of developing radiopharmaceutical kits [5].

Blood pool imaging (BPI) radiopharmaceuticals are used for the study of circulation patterns in various diseases, usually injected intravenous/arterially without considerable leakage into the interstitial space and high retention in the circulation. ^{99m}Tc-labeled red blood cells (^{99m}Tc-RBC) was used previously however, not very popular now due to risks on blood handling. Subsequently, ^{99m}Tc-labeled natural and artificial polymers were introduced, suffering from limited spatial resolution as single photon emission computed tomography (SPECT) agents as well as toxicity.

To benefit from the advantages of PET, several positron emitter blood-pool tracers were introduced. Some required blood cell handling and some were limited by their very short half-life. Table 1, summarizes a list of BPI tracers with their properties.

On the other hand, ^{68}Ga-polymers are favorable due to facile chemistry of Ga-68, availability (*via* ^{68}Ge/^{68}Ga generators as well as direct cyclotron production [19]) and possible development of radiopharmaceutical kits [20].

Dextran (DXT) is a water-soluble bacterial polysaccharide, consisting of α-(1-6)–linked glucan with different ratios of the side chains attached mainly to the 3-positions and occasionally to the 1 or 4-positions of the D-glucose units backbone [21]. It has been conjugated with chelating agents for metal labeling for development of MRI agnents [22], therapeutic radiopharmaceuticals (^{188}Re-cysteine DXT) [23] as well as ^{99m}Tc-BPI agents (See Table 1).

Table 1: Characteristic of selected BPI tracers.

Tracers	Half life	Imaging	Advantage(s)	Limitation(s)	Ref.
^{99m}Tc-RBC	6.6 h	SPECT	Radionuclide availability	Microbial risks, low spatial resolution	[6]
^{99m}Tc-HSA derivaties	6.6 h	SPECT	Radionuclide availability	Limited spatial resolution	[7]
^{99m}Tc-ethylene glycols	6.6 h	SPECT	Radionuclide availability	Limited spatial resolution	[8]
^{67}Ga-polyglycerols	3.21 days	SPECT	Long imaging studies	Dosimetry concerns, limited spatial resolution	[9]
^{11}C-CO–RBC	20.3 min	PET	High spatial resolution	Short half-life, availability of cyclotrons, microbial risks	[10]
^{62}Cu-HSA	9.7 min	PET	High spatial resolution	Short half-life, availability	[11]
^{18}F-HSA	109 min	PET	High spatial resolution, suitable half life	Complicated labeling, availability of cyclotrons	[12]
^{68}Ga- HSA	68 min	PET	Generator availability, high spatial resolution, suitable half life	Conjugation chemistry	[13]
^{18}F-FDG-RBC	109 min	PET	High spatial resolution	Microbial risks, availability of cyclotrons	[14]
^{99m}Tc-mannosylated cysteine DXT	6.6 h	SPECT	Radionuclide availability	Limited spatial resolution	[15]
^{99m}Tc-DTPA/MAG_3-Mannosyl-DXT	6.6 h	SPECT	Radionuclide availability	Limited spatial resolution	[16]
^{68}Ga-NOTA mannosylated DXT	68 min	PET	Generator availability, high spatial resolution, suitable half life	Conjugation chemistry	[17]
^{68}Ga-DXT	68 min	PET	Generator availability, high spatial resolution, suitable half life	Colloid formation	[18]

HSA, Human serum albumin; DXT, dextran; DTPA, diethylenetriamine pentaacetic acid; NOTA, 1,4,7-tricarboxymethyl-1,4,7-triazacyclononane.

Recently attempts for developing a favorable ^{68}Ga-DXT complex were not successful at pH. 4–5, although a ^{68}Ga-DXT complex was formed at pH. 9 in high yield [18], showing high lung accumulation after *i.v.* injection possibly due to the formation of colloids. In this work, a modified water soluble DXT structure is developed for ^{68}Ga-labeling under milder conditions suitable for ready-to-use kits. Consecutive oxidation of vicinal hydroxyl groups in DXT structure results in formation of dextran carboxylates ($DXT(COOH)_n$) [17, 24] followed by purification, structure characterization, solubility and cytotoxicity tests. Finally, ^{68}Ga-$DXT(COOH)_n$ derivatives were prepared and *in vitro* and post-mortem preclinical studies of the radiocomplex performed in wild type male rats.

2 Materials and methods

The ^{68}Ge/^{68}Ga generator (30 mCi/day activity) was obtained from *Pars Isotope Co. Karaj, Iran*. DXT (MW = 35–45 kDa) was purchased from Sigma-Aldrich (Germany). The ^{68}Ge/^{68}Ga generator was eluted with 0.2 N HCl solution to get an acidic solution of [^{68}Ga]$GaCl_3$. Peracetic acid (38–40 % solution in water) and sodium bromide were purchased from Merck-Millipore, Germany. A digital hot-pot heater (Turkey) was used to heat vials at a defined temperature. A miniGita radio-TLC scanner equipped with Gina-star software, Raytest, Germany was used to plot TLC radio chromatograms. The gel filtration chromatography (GPC) was done on an Agilent 1100 HPLC system equipped with a reflective index detector (RID) and a PL aquagel-OH, 8 µm MIXED-H, 300 × 7.5 mm column. A Perkin Elmer Spectrum Two IR spectrometer was used to plot IR spectrums. All animal studies were conducted based on the ethical guidelines in accordance with the National Institutes of Health guide for the care and use of laboratory animals (NIH Publications No. 8023, revised 1978).

2.1 Synthesis and characterization DXT-aldehyde ($DXT(CHO)_n$) (2)

Oxidation of DXT vicinal hydroxyl groups to the aldehyde was performed using $NaIO_4$ according to previously reported method with slight modifications [22]. Briefly, DXT (1.6 g, 10 mM of glucose units) (**1**) was dissolved in

15 mL of sodium acetate buffer (0.1 M, pH. 6) and sodium metaperiodate was added in molar ratios of 1:10, 3:10 and 5:10 (IO_4^-/glucose unit) to yield theoretical oxidation degrees of 10, 30 and 50 %. The mixture was stirred at 4 °C in darkness for 20 h. The reaction was quenched by the addition of ethylene glycol. The oxidized DXT derivatives were dialyzed against ultrapure water using a dialysis tube (Sigma-Aldrich, MWCO = 12.400 kDa) for 2 days. The final product was freeze-dried to obtain white powder. Formation of aldehyde functional groups was confirmed by FT-IR. The percent degrees of oxidation (DO%) was determined using hydroxylamine hydrochloride test comparing with native DXT as a reference [25].

2.2 Synthesis and characterization of DXT-carboxylate (DXT(COOH)$_n$) (3)

Through further oxidation of the aldehyde derivative **2**, DXT(COOH)$_n$ was synthesized according to the previously reported method [24]. Briefly, 1 g samples of aldehyde DXT derivative [DO% (approximate mM of the aldehyde group); 8.3 (1.02 mmol), 24.6 (3.03 mmol) and 39.8 (4.91 mmol)] were dissolved in 30 mL of acetate buffer (0.1 M, pH.6) in three separate glass flasks. Then sodium bromide (1 mM, 5 mL) and peracetic acid (38–40 % w/w) with various amounts (0.190, 0.565 and 0.925 mL equivalent to 1.1, 3.3 and 5.4 mmol, respectively) were added to each flask. The flasks were tightly closed and stirred in dark for 12 h. The pH was then adjusted to 8.0 and the sodium salt solutions of DXT-carboxylates were dialyzed against ultrapure water for 48 h using dialysis tubes (MWCO = 12.4 kDa). The dialysis continued against 0.01 M HCl solution and ultrapure water, respectively to afford acidic form (**3**) followed by lyophilization and FT-IR spectroscopy. The carboxylic acid contents were determined by colorimetric titration of the products against 0.1 M NaOH/phenolphthalein. The DXT(COOH)$_n$, DXT(CHO)$_n$ and DXT molecular weights were determined by GPC (ultra-pure water as eluent; 1 mL/min) using DXT standards (MWs:5.2–668 kDa).

2.3 Determination of dissolution rates for DXT, DXT(CHO)$_n$ and di-DXT(COOH)$_n$ derivatives

In order to confirm water solubility of DXT derivatives, dissolution rates were determined in aqueous solutions according to reported method [26]. Briefly, 10 % w/w solutions of samples were prepared in ultra-pure water. Aliquots of 1 mL were divided into small glass vials, frozen at –20 °C and freeze-dried, to get similar dried samples. To each sample, 0.8 mL of ultrapure water was added and the dissolution time was recorded at 37 °C (n = 3).

2.4 MTT cytotoxicity assay

The cytotoxicity of native DXT, DXT(CHO)$_n$ and DXT(COOH)$_n$ with different degrees of oxidation were assessed by 3-[4, 5-dimethylthiazol-2-yl]-2, 5-diphenyl tetrazolium bromide (MTT) assay. HeLa cell line was purchased from the National Cell Bank, Iran. The cells were cultured in 75 cm^2 cell culture flasks and scraped off, centrifuged for 5 min at 1100 g, resuspended in the RPMI-1640 mediums (Cambrex Bioscience), and finally counted by Trypan Blue exclusion (99 % viability). The cell concentration was adjusted to 10^5 cells/mL with fresh medium and maintained at 37 °C in a humidified incubator with 5 % CO_2 atmosphere. Stock solutions of samples were prepared in the RPMI-1640 medium (5000 µg/mL). The sample concentrations of 5000–4.8 µg/mL (V = 50 µL in each well) was obtained by serial dilution using the fresh medium. Subsequently, 50 µL aliquot of cell suspension was added to each well and the plates were incubated at 37 °C and with 5 % CO_2 atmosphere. The fresh medium was used as the control test. The final samples concentrations in the test were 2500–2.4 µg/mL. Twenty four hours after incubation, MTT solution (USB Corporation, Cleveland, OH, USA) was added to each well and the plates were incubated for 4 h at 37 °C. The MTT solution was removed, and DMSO was added to dissolve formazan crystals. The absorbance at 540 nm was read on a 680 Microplate Reader (Bio-Rad Laboratories, Hercules, CA, USA). The percentage of viability was calculated as AT/AC × 100, where AT and AC are the absorbance of treated and control cells, respectively.

2.5 Preparation of ^{68}Ga-DXT(COOH)$_n$ derivatives with varios DOs (4)

^{68}Ge/^{68}Ga generator was eluted with 0.2 M HCl solution, and 0.5 mL fractions were collected. The fractions 2–4, with maximum radioactivities, were transferred to a 10 mL borosilicate pyrogen-free vial (550 MBq) and heated to dryness at 50–60 °C under an N_2 gas stream followed by the addition of ammonium acetate solution (500 µL, 0.5 mol/L, pH = 5.0). The resulted solution was checked for the radiochemical purity using Whatman No 1 paper and 50 mmol/L DTPA (pH = 5.0) solution as the mobile

phase [27]. Then, 0.5 mL of the 2.5, 5, 10 and 20 mg/mL of DXT(COOH)$_n$ solutions (with various DO%) were added to ^{68}Ga solutions and the mixtures were heated at 90 °C up to 1 h. The radiochemical purities were assessed by TLC-SG (part number: 105554, Merck, Darmstadt, Germany) and DTPA solution (10 mmol/L, pH = 5.5) as the mobile phase. In this system, [^{68}Ga]Ga(OH)$_3$ colloids, ^{68}Ga-cation (as DTPA complex), and the ^{68}Ga-DXT(COOH)$_n$ had R_f values of 0.0, 0.8 and 0.4, respectively. The final solution was passed through a 0.22 μ microbial filter.

2.6 Stability studies

The *in vitro* stability of ^{68}Ga-DXT(COOH)$_n$ with various DOs was assessed in the storage solution, cysteine, and human blood serum at different intervals; 30, 60, 90 and 120 min. The complex solution (pH = 7) was stored at room temperature, and its radiochemical purity was measured based on the TLC analysis as described above. To assay transchelation of ^{68}Ga from the DXT(COOH)$_n$ to the cysteine, a mixture of 4 and cysteine solution ($C_{ligand}/C_{cysteine}$ = 1/100) was incubated at 37 °C for 2 h. Aliquots (10 μL) were tested to determine instability products by TLC (methanol as mobile phase). In this system, ^{68}Ga-DXT(COOH)$_n$ remain at origin while ^{68}Ga-cysteinate migrates to R_f = 0.6. The stability of radioactive complex in serum was investigated by incubating equal volumes of complex and fresh serum at 37 °C and screening for radiochemical purity by thin layer chromatography on TLC-SG and normal saline as mobile phase. The radiolabeled components of serum remain at the origin, while ^{68}Ga-DXT(COOH)$_n$ migrates to R_f = 0.4.

2.7 Biodistribution studies

The biodistribution of ^{68}Ga-DXT(COOH)$_n$ derivatives (**4**) with acceptable stability among organs (blood, liver, lung, spleen, kidneys, bladder, stomach, small intestine, large intestine, femur bone, rib bone, knee, muscle, urine and feces) was determined in the healthy wild-type male rats by tissue sampling and presented as injected dose per gram (ID/g) of organs. Solid tissues were rinsed gently, but thoroughly with normal saline to remove remaining traces of blood before wheithing and counting. The sterile solutions of **4** (~6.6 MBq; DO = 24.6 and 39.8 %) were injected separately into tail vein of rats (n = 3 for each time interval) under ketamine-xylazine anesthesia. The animals were sacrificed by CO_2 asphyxiation at 30, 60, 90 and 120 min after injection. The tissues samples were weighed and counted for radioactivity in a gamma counter equipped with a 2-inch sample holder.

3 Result and discussion

3.1 Synthesis and characterization of ^{68}Ga-DXT(CHO)$_n$ (2)

DXT structure consists of vicinal triols on the C_2, C_3, and C_4 of the α-(1-6)-linked glucose units. As shown in Figure 1,

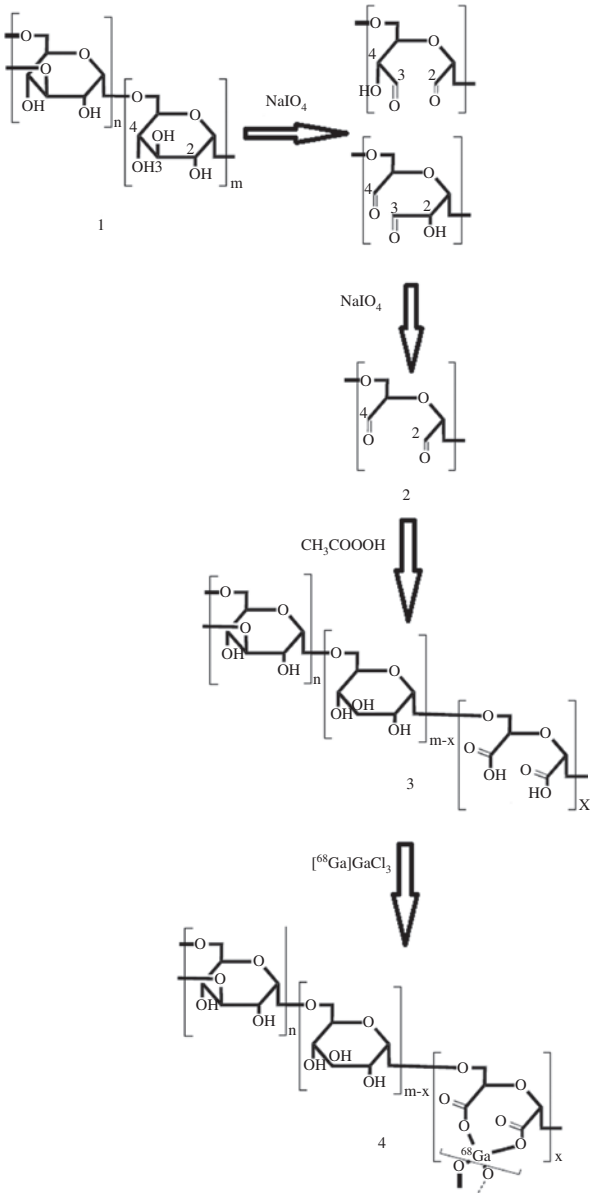

Figure 1: Syntheses of DXT derivatives, DXT(CHO)$_n$ (2), DXT(COOH)$_n$ (3) and final complex ^{68}Ga-DXT(COOH)$_n$ (**4**).

the metaperiodate cleavage-oxidation reaction could take place either on the C_2–C_3 or C_3–C_4 bonds to form a *di*-aldehyde residue. Further, in the presence of oxidant agent, second cleavage reaction could take place on the C_3 aldehyde moiety and vicinal hydroxyl on C_2 or C_4 to yield a doubly oxidized product [28]. Figure 2 presents the FT-IR spectrums of the native DXT and synthesized DXT derivatives. The characteristic peak at 1726 cm^{-1} on FT-IR spectrum confirms the aldehyde groups [29]. The degrees of oxidation were calculated based on hydroxylamine hydrochloride test and summarized in Table 2.

3.2 Synthesis and characterization of DXT(COOH)$_n$

The aldehyde groups of DXT(CHO)$_n$ were oxidized to the carboxylate groups. The FT-IR stretch band for hydroxyl groups of DXT(COOH)$_n$ was observed in the range of 2900–3600 cm^{-1} (Figure 2). This different shaped broad band belongs to the OH groups of both carboxyl moiety and non-oxidized alcoholic groups of the DXT backbone. Furthermore, a new strong and sharp peak in the 1742 cm^{-1} confirms the C=O stretch of carboxyl groups. The band at 1647 cm^{-1} belongs to overtone and combination bands of the alcoholic hydroxyl groups of DXT backbone. The titration results reveal carboxyl contents of 1.01, 3.07 and 4.92 mmol/g. The change in the molecular weight of DXT in the oxidation reactions was assessed by GPC and summarized in Table 2. As expected the molecular weight of DXT has decreased.

3.3 Dissolution rate of DXT and its derivatives

Linear relationship between the solubility and dissolution rate of the materials has been shown previously [30] and for solubility comparison of the DXT derivatives, dissolution times were recorded. Figure 4 demonstrates longer disulotion time for DXT(CHO)$_n$ compared to native DXT. Furthermore, the dissolution time was longer for higher degree of oxidation of the DXT(CHO)$_n$. However, DXT(COOH)$_n$ showed

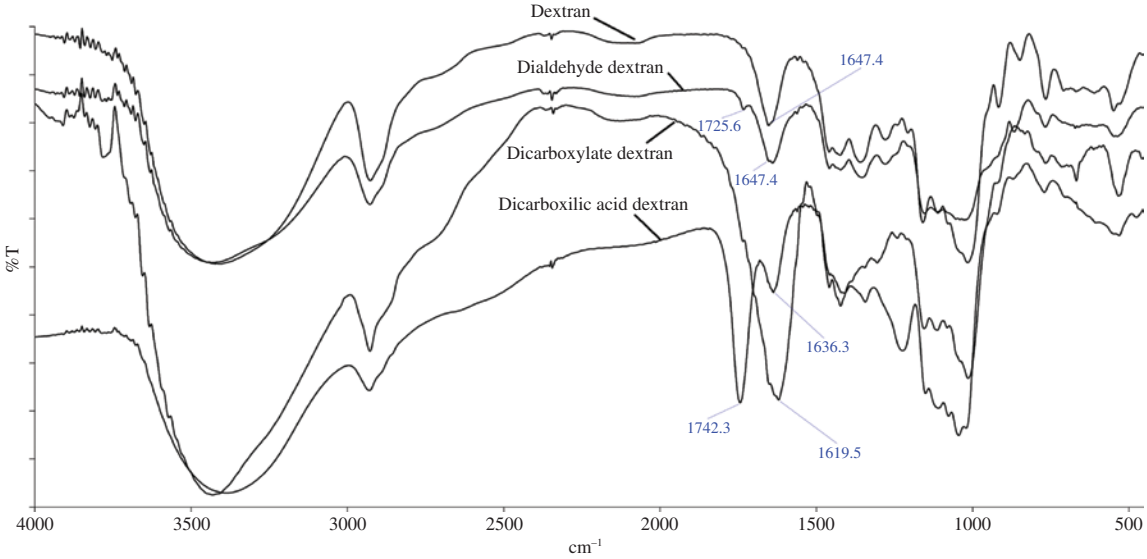

Figure 2: FT-IR spectra for DXT, DXT(CHO)$_n$ and DXT(COOH)$_n$ derivatives.

Table 2: DXT oxidation conditions and product specifications.

Reaction	$NaIO_4$/glucose units ratio	Degree of oxidation %	MW of DXT(CHO)$_n$ (kDa)	MW of DXT(COOH)$_n$ (kDa)
1	1:10	8.3	33.2–45.4	32.6–43.1
2	3:10	24.6[a]	30.3–41.1	29.8–37.9
3	5:10	39.8	27.8–39.0	26.9–35.6

[a]GPC elution chromatogram for DXT, *di*-aldehyde DXT and relevant DXT(COOH)n was presented in Figure 3.

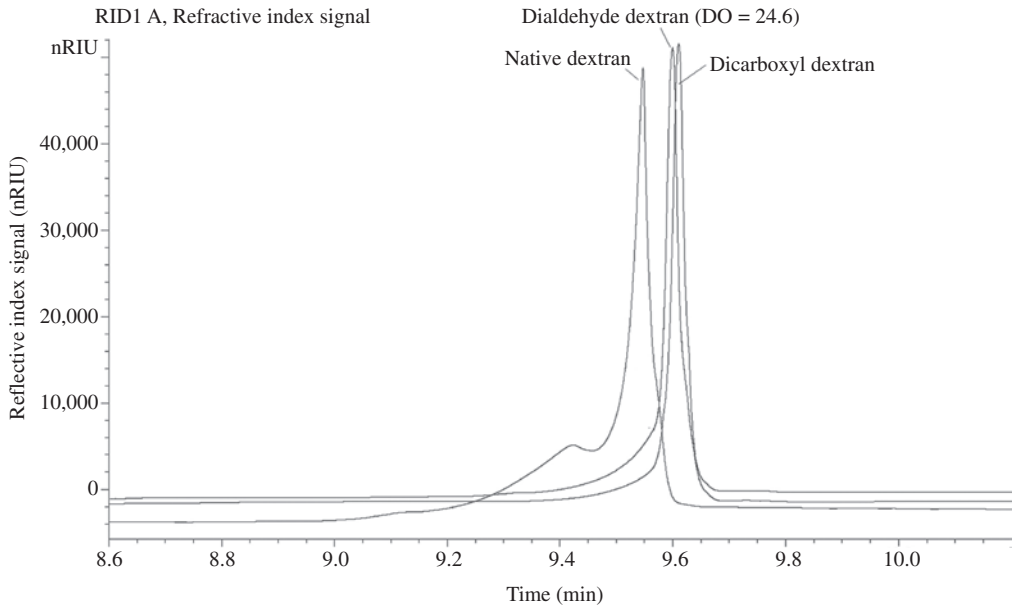

Figure 3: GPC elution chromatogram for DXT, DXT(CHO)$_n$ (DO = 24.6 %) and relevant DXT(COOH)$_n$.

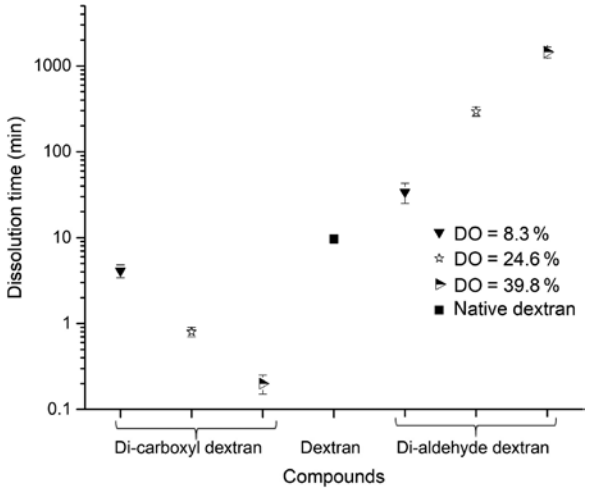

Figure 4: Dissolution rate profile of DXT and its derivatives.

significant shorter dissolution time, which became shorter by the increasing carboxylate content.

3.4 MTT cytotoxicity assay

Although native DXT is known to be a non-toxic polymer [31], several publications reported the cytotoxicity of DXT(CHO)$_n$ [32]. Due to the high chemical reactivity of the aldehyde group, DXT(CHO)$_n$ has been modified to various derivatives such as reduced DXT, ethanol-amine DXT, ethanol-imine DXT and acetal DXT. All mentioned derivatives have shown less toxicity than DXT(CHO)$_n$. The cytotoxicity of the native DXT, the DXT(CHO)$_n$ (DO = 8.3, 24.6 and 39.8 %) and the respective DXT(COOH)$_n$ was investigated against Hella cell line. As shown in Figure 5 the native DXT did not affect the cell growth, however after incubation for 24 h, DXT(CHO)$_n$ (DO = 8.3, 24.6 and 39.8 %) decreased the cell viability with CV_{50} of approximate 27, 9.5 and 5.5 µg/mL, respectively. The results are in agreement with previous reports on the cytotoxicity of DXT(CHO)$_n$. Incubation of Hella cells with DXT(COOH)$_n$ samples resulted in a slight decrease in the cell viability corelated with concentration used and carboxylate

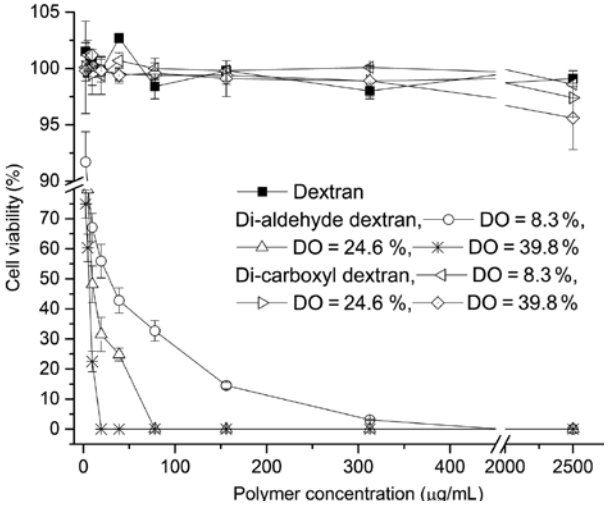

Figure 5: MTT cytotoxicity profile of DXT and its derivatives on HeLa cell line.

group content. After 24-h incubation of cells with DXT(COOH)$_n$ solutions (2500 µg/mL), cell viability was decreased to 98.6, 97.4 and 95.6 % for relevant derivatives with DO = 8.3, 24.6 and 39.8 %, respectively. Thus, DXT(COOH)$_n$ demonstrated insignificant cytotoxicity compared to native DXT.

3.5 Radiolabeling of DXT(COOH)$_n$

Since no macroscopic chelation work at the cold chemistry level has been performed in this work, the chelation of Ga with the carboxylate moieties introduced in the dextran is extrapolated only from the increase in the labeling yield. Figure 6a–c presents the effect of DXT(COOH)$_n$ sample concentration, the degree of oxidation and the radiolabeling time on the radiolabeling yield (decay corrected). In general, DXT(COOH)$_n$ showed a higher radiolabeling capability compared to native DXT at pH. 5.0 at 90 °C. In addition, the radiolabeling efficiency increased with the degree of oxidation and carboxylate content of products. Labeling efficiency reached up to 95 % for the *di*-carboxylic acid DXT (DO = 8.3 %) at ≥5 mg/mL and >30 min heating. However, radiolabeling efficiencies of >98 % were obtained only >2.5 mg/mL solutions of derivatives (DO = 24.6 and 39.8 %) and 10 min heating. The results demosntrate the direct involvement of carboxilate moieties in Ga-68 chelating.

3.6 Stability studies

Figure 7a–c demonstrates the radiochemical purities of complexes in final samples, in presence of cysteine and human serum. After 120 min, the ^{68}Ga-DXT(COOH)$_n$ **4** remained intact in final solution. On the other hand, the radiochemical purities decreased in presence of cysteine and human serum while the complexes with higher carboxylate content showed better stability. For instance, the radiochemical purity of [^{68}Ga]-DXT(COOH)$_n$ (DO = 24.6 and 39.8 %) remained >85 %. ^{68}Ga-DXT complex showed higher stability in serum than cysteine solution (not shown see [21]). This can be explained by the fact that colloidal Ga-DXT complex is resistant to the release of radionuclide from the colloid network. On the other hand, the ^{68}Ga-DXT(COOH)$_n$ complex showed slightly lower stability in serum compared to ^{68}Ga-DXT possibly due to higher solubility and easier trans-chelation to serum proteins (such as transferrin). However, the release is very slight and complex is majorly (>90 %) intact in 120 min.

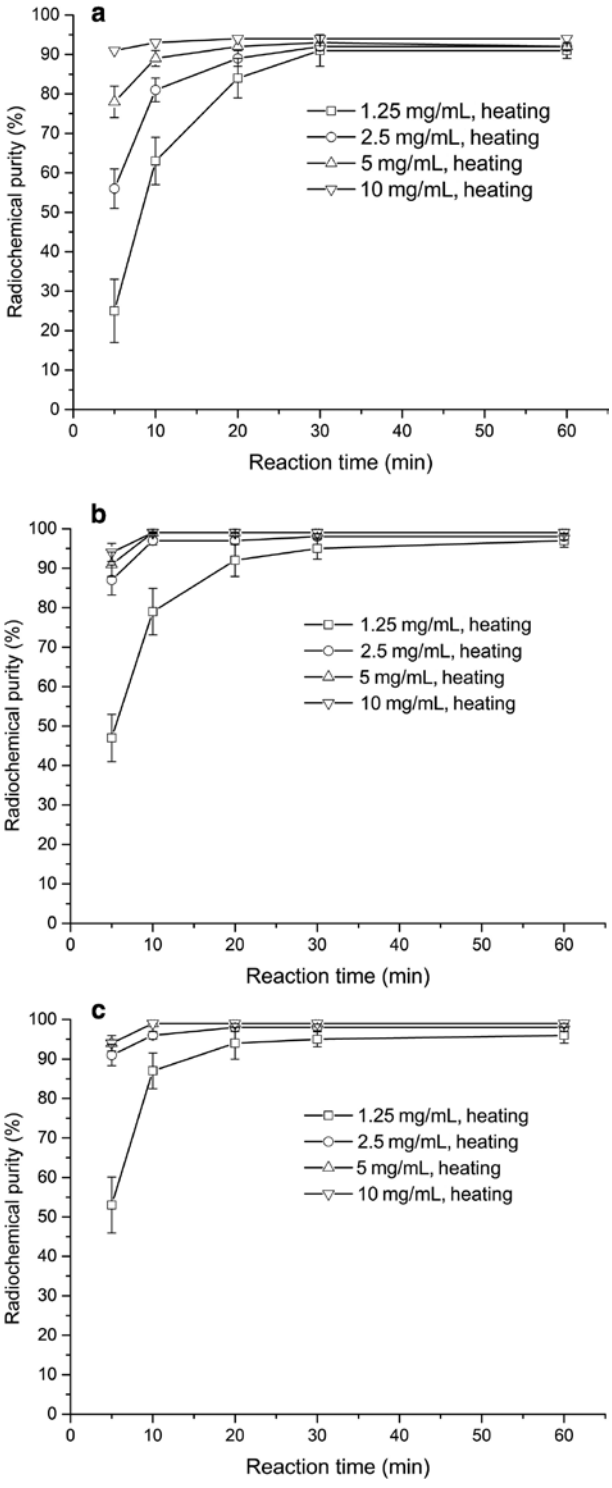

Figure 6: Effects on the radiolabeling yield.
Radiolabeling efficiencies of DXT(COOH)$_n$ with ^{68}Ga: (a) DO = 8.3 %, (b) DO = 24.6 %, and (c) DO = 39.8 %.

3.7 Biodistribution studies

All three synthesized DXT(COOH)$_n$ derivatives with different carboxylation levels were successfully radiolabeled.

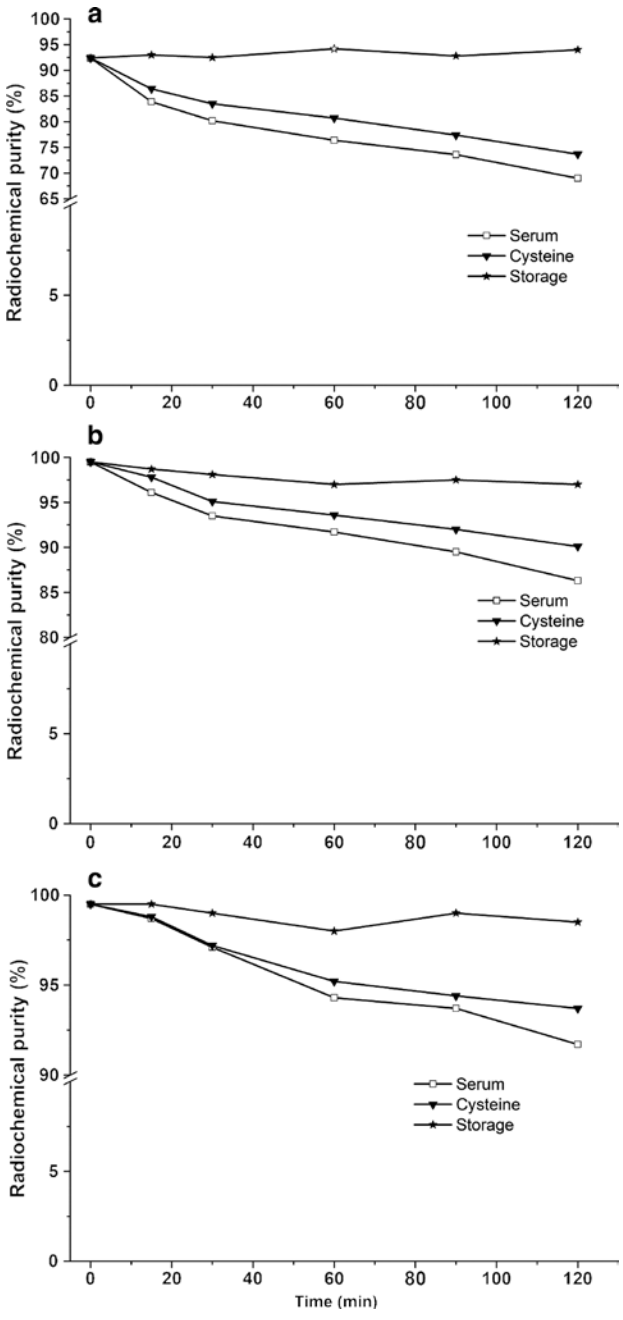

Figure 7: Stability of the ^{68}Ga-DXT(COOH)$_n$ samples in the storage condition and toward cysteine and human serum.
Each point represents an average of three measurements.
(a) DO = 8.3 %, (b) DO = 24.6%, and (c) DO = 39.8%.

However, in case of DO = 8.3 % derivative, the stability during *in vitro* studies decreased significantly (70 % in 2 h), so it was excluded from biodistribution studies.

Figure 8a and b shows the biodistribution profiles of ^{68}Ga-DXT(COOH)$_n$ (DO = 24.6 and 39.8 %). For both derivatives, the highest accumulations are in the blood, kidneys and bladder indicating suitable blood pool retention of the complexes and urine pathway excretion.

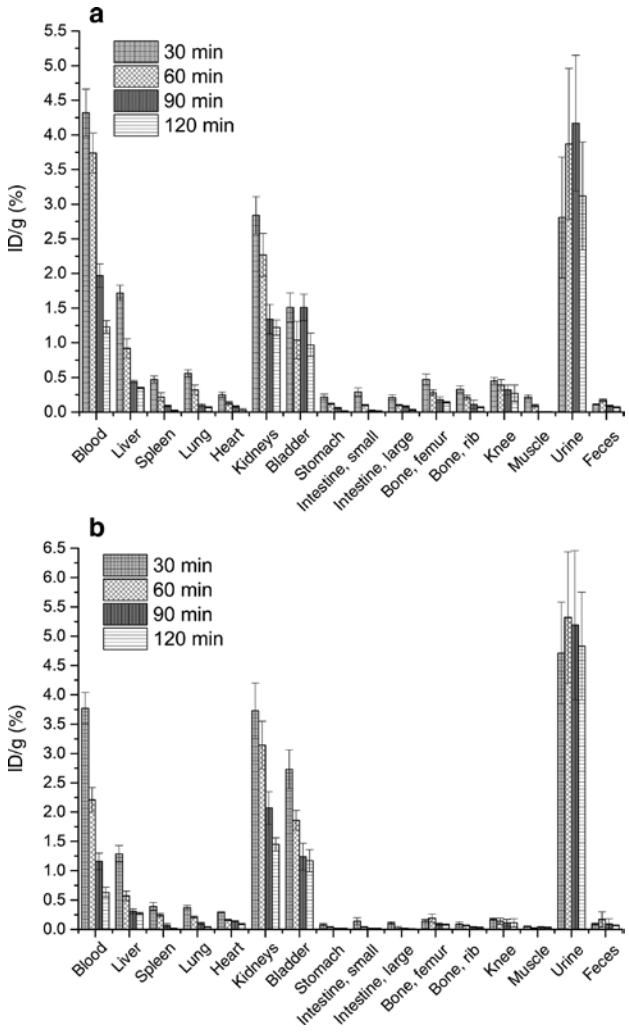

Figure 8: Biodistribution profile of the ^{68}Ga-DXT(COOH)$_n$ derivatives in normal rats.
(a) DO = 24.6%, and (b) DO = 39.8 %.

However, the clearance rate of radioactivity from the blood for derivative with DO = 39.8 %, is faster possibly due to higher hydrophilicity, anionic surface and decrease in molecular weight (during oxidation step). Significant accumulations were observed in the liver, lungs and knee joints. Interestingly, ^{68}Ga-dicarboxlyate DXT had a lower uptake in the lungs and liver and a higher uptake in kidneys compared to ^{68}Ga-DXT [21]. These results are also possibly related to higher water solubility of ^{68}Ga-DXT(COOH)$_n$ in water and/or decrease in the molecular weight decrease [29].

4 Conclusions

To improve the properties of the ^{68}Ga-DXT as a blood pool agent, ^{68}Ga-DXT(COOH)$_n$ derivative was developed. DXT

was oxidized by $NaIO_4$ (molar ratios of 1:10, 3:10 and 5:10 of IO_4^-/glucose unit) followed by peracetic acid oxidation to yield low toxicity, water-soluble di-carboxylate DXTs with different carboxylate moieties per molecule. All derivatives were successfully labeled with ^{68}Ga (radiolabeling efficiency >90 %). Among those, a product with highest oxidation degree showed better chelating capability and stability *in vitro*. After intravenous administration, ^{68}Ga-DXT(COOH)$_n$ mainly retained in the blood circulation and excreted from the urinary pathway majorly. A lower uptake was observed in the lungs compared to ^{68}Ga-DXT. Compared to previously developed agents for blood pool imaging, ^{68}Ga-DXT(COOH)$_n$ shows similar accumulation profile in the blood, faster renal clearance and low toxicity suggesting usefulness for blood pool imaging. More studies are required for the use of other modified DXT derivatives to meet all requirements for an ideal blood pool imaging agent such high radiolabeling efficiency, longer retention circulation and low toxicity.

Acknowledgements: This research has been supported by Tehran University of Medical Sciences (TUMS), Funder Id: http://dx.doi.org/10.13039/501100004484, grant 94-02-58-29793.

References

1. Mossine, A. V., Thompson, S., Brooks, A. F., Sowa, A. R., Miller, J. M., Scott, P. J.: Fluorine-18 patents (2009–2015). Part 2: new radiochemistry. Pharm. Pat. Anal. **5**(5), 319 (2016).
2. Follacchio, G. A., De Feo, M. S., De Vincentis, G., Monteleone, F., Liberatore, M.: Radiopharmaceuticals labelled with copper radionuclides: clinical results in human beings. Curr. Radiopharm. **11**(1), 22 (2018).
3. van Es, S. C., Brouwers, A. H., Mahesh, S. V. K., Leliveld-Kors, A. M., de Jong, I. J., Lub de Hooge M. N., de Vries, E. G. E., Gietema, J. A., Oosting, S. F.: 89Zr-Bevacizumab PET: potential early indicator of everolimus efficacy in patients with metastatic renal cell carcinoma. J. Nucl. Med. **58**, 905 (2017).
4. Brasse, D., Nonat, A.: Radiometals: towards a new success story in nuclear imaging? Dalton Trans. **44**, 4845 (2015).
5. Fani, M., André, J. P., Maecke, H. R.: 68Ga-PET: a powerful generator-based alternative to cyclotron-based PET radiopharmaceuticals. Contrast Media. Mol. Imaging. **3**, 53 (2008).
6. Front, D., Israel, O., Groshar, D., Weininger, J.: Technetium-99m-labeled red blood cell imaging. Semin. Nucl. Med. **14**, 226 (1984).
7. Henze, E., Robinson, G. D., Kuhl, D. E., Schelbert, H. R.: Tc-99m dextran: a new blood-pool-labeling agent for radionuclide angiocardiography. J. Nucl. Med. **23**, 348 (1982).
8. Bogdanov, A. A., Callahan, R. J., Wilkinson, R. A., Martin, C., Cameron, J. A., Fischman, A. J., Brady, T. J., Weissleder, R.: Synthetic copolymer kit for radionuclide blood-pool imaging. J. Nucl. Med. **35**, 1880 (1994).
9. Saatchi, K., Gelder, N., Gershkovich, P., Sivak, O., Wasan, K. M., Kainthan, R. K., Brooks, D. E., Häfeli, U. O.: Long-circulating non-toxic blood pool imaging agent based on hyperbranched polyglycerols. Int. J. Pharm. **422**, 418 (2012).
10. Cross, S. J., Lee, H. S., Metcalfe, M. J., Norton, M. Y., Evans, N. T., Walton, S.: Assessment of left ventricular regional wall motion with blood pool tomography: comparison of 11CO PET with 99Tcm SPECT. Nucl. Med. Commun. **15**, 283 (1994).
11. Mathias, C. J., Welch, M. J., Green, M. A., Diril, H., Meares, C. F., Gropler, R. J., Bergmann, S. R.: In vivo comparison of copper blood-pool agents: potential radiopharmaceuticals for use with copper-62. J. Nucl. Med. **32**, 475 (1991).
12. Basuli, F., Li, C., Xu, B., Williams, M., Wong, K., Coble, V. L., Vasalatiy, O., Seidel, J., Green, M. V., Griffiths, G. L., Choyke, P. L., Jagoda, E. M.: Synthesis of fluorine-18 radio-labeled serum albumins for PET blood pool imaging. Nucl. Med. Biol. **42**, 219 (2015).
13. Hoffend, J., Mier, W., Schuhmacher, J., Schmidt, K., Dimitrakopoulou-Strauss, A., Strauss, L. G., Eisenhut, M., Kinscherf, R., Haberkorn, U.: Gallium-68-DOTA-albumin as a PET blood-pool marker: experimental evaluation in vivo. Nucl. Med. Biol. **32**, 287 (2005).
14. Matsusaka, Y., Nakahara, T., Takahashi, K., Iwabuchi, Y., Nishime, C., Kajimura, M.: Jinzaki: M118F-FDG-labeled red blood cell PET for blood-pool imaging: preclinical evaluation in rats. EJNMMI Res. **7**(1), 19 (2017).
15. Pirmettis, I., Arano, Y., Tsotakos, T., Okada, K., Yamaguchi, A., Uehara, T., Morais, M., Correia, J. D. G., Santos, I., Martins, M., Pereira, S., Triantis, C., Kyprianidou, P., Pelecanou, M., Papadopoulos, M.: New (99m)Tc(CO)(3) mannosylated dextran bearing S-derivatized cysteine chelator for sentinel lymph node detection. Mol. Pharm. **9**, 1681 (2012).
16. Hoh, C. K., Wallace, A. M., Vera, D. R.: Preclinical studies of [99mTc]DTPA-mannosyl-dextran. Nucl. Med. Biol. **30**, 457 (2003).
17. Tsoukalas, C., Lazopoulos, A., Boschetti, F., Triantis, C., Bouziotis, P., Pelecanou, M., Papadopoulos, M., Pirmettis, I.: Labeling of a NOTA mannosylated dextran with 68Ga. Nucl. Med. Biol. **41**, 801 (2014).
18. Gholipour, N., Akhlaghi, M., Kheirabadi, A. M., Beiki, D., Geramifar, P., Yousefnia, H., Mazidi, M.: Chelator-free radiolabeling of dextran with 68Ga for PET studies. J. Radioanal. Nucl. Chem. **311**(3), 1811 (2017).
19. Pharmeuropa 30.4, Reference: PA/PH/Exp. 14/T (18) 13 ANP; GALLIUM (68Ga) CHLORIDE (ACCELERATOR-PRODUCED) SOLUTION FOR RADIOLABELLING (draft).
20. Rösch, F.: Past, present and future of 68Ge/68Ga generators. Appl. Radiat. Isot. **76**, 24 (2013).
21. Varshosaz, J.: Dextran conjugates in drug delivery. Expert Opin. Drug Deliv. **9**, 509 (2012).
22. Duarte, M. G., Geraldes, C. F. G. C., Peters, J. A., Gil, M. H.: Preparation of dextran-based macromolecular chelates for magnetic resonance angiography. In: Biorelated Polymers. Springer US, Boston, MA (2001).
23. Du, J., Marquez, M., Hiltunen, J., Nilsson, S., Holmberg, A. R.: Radiolabeling of dextran with rhenium-188. Appl. Radiat. Isot. **53**, 443 (2000).
24. Haaksman, I. K., Besemer, A. C., Jetten, J. M., Timmermans, J. W., Slaghek, T. M.: The oxidation of the aldehyde groups in dialdehyde starch. Starch **58**, 616 (2006).

25. Heindel, N. D., Zhao, H., Leiby, J., VanDongen, J. M., Lacey, C. J., Lima, D. A., Shabsoug, B., Buzby, J. H.: Hydrazide pharmaceuticals as conjugates to polyaldehyde dextran: syntheses, characterization, and stability. Bioconjug. Chem. **1**, 77 (1990).
26. Guo, M. Q., Hu, X., Wang, C., Ai, L.: Polysaccharides: structure and solubility. In: S. Xu (Ed.), Solubility of Polysaccharides (2017), InTech, Croatia, p. 7.
27. Mirzaei, A., Jalilian, A. R., Shabani, G., Fakhari, A., Akhlaghi, M., Beiki, D.: Development of 68Ga ethyl cysteinate dimer for PET studies. J. Radioanal. Nucl. Chem. **307**(1), 725 (2016).
28. Maia, J., Carvalho, R. A., Coelho, J. F. J., Simões, P. N., Gil, M. H.: Insight on the periodate oxidation of dextran and its structural vicissitudes. Polymer (Guildf). **52**, 258 (2011).
29. Azzam, T., Raskin, A., Makovitzki, A., Brem, H., Vierling, P., Michal, L., Abraham, J.: Cationic polysaccharides for gene delivery. Macromolecules **35**, 9947 (2002).
30. Issa, M. G., Ferraz, H. G.: Intrinsic dissolution as a tool for evaluating drug solubility in accordance with the biopharmaceutics classification system. Dissolut. Technol. **18**, 6 (2011).
31. Dhaneshwar, S., Kandpal, M., Gairola, N., Kadam, S., Kadam, S.: Dextran: a promising macromolecular drug carrier. Indian J. Pharm. Sci. **68**, 705 (2006).
32. Sokolsky-Papkov, M., Domb, A. J., Golenser, J.: Impact of aldehyde content on amphotericin B-dextran imine conjugate toxicity. Biomacromolecules **7**, 1529 (2006).